

# miR-661 downregulates both Mdm2 and Mdm4 to activate p53

Y Hoffman<sup>1,2,3</sup>, DR Bublik<sup>2,3</sup>, Y Pilpel<sup>\*1</sup> and M Oren<sup>\*2</sup>

The p53 pathway is pivotal in tumor suppression. Cellular p53 activity is subject to tight regulation, in which the two related proteins Mdm2 and Mdm4 have major roles. The delicate interplay between the levels of Mdm2, Mdm4 and p53 is crucial for maintaining proper cellular homeostasis. microRNAs (miRNAs) are short non-coding RNAs that downregulate the level and translatability of specific target mRNAs. We report that miR-661, a primate-specific miRNA, can target both *Mdm2* and *Mdm4* mRNA in a cell type-dependent manner. miR-661 interacts with *Mdm2* and *Mdm4* RNA within living cells. The inhibitory effect of miR-661 is more prevalent on Mdm2 than on Mdm4. Interestingly, the predicted miR-661 targets in both mRNAs reside mainly within Alu elements, suggesting a primate-specific mechanism for regulatory diversification during evolution. Downregulation of Mdm2 and Mdm4 by miR-661 augments p53 activity and inhibits cell cycle progression in p53-proficient cells. Correspondingly, low miR-661 expression correlates with bad outcome in breast cancers that typically express wild-type p53. In contrast, the miR-661 locus tends to be amplified in tumors harboring p53 mutations, and miR-661 promotes migration of cells derived from such tumors. Thus, miR-661 may either suppress or promote cancer aggressiveness, depending on p53 status.

*Cell Death and Differentiation* (2014) 21, 302–309; doi:10.1038/cdd.2013.146; published online 18 October 2013

p53 is a transcription factor that responds to diverse types of stress and modulates the expression of a large group of genes regulating cell cycle progression, cell death and survival, metabolic homeostasis, genomic integrity, differentiation and more.<sup>1,2</sup> The p53 pathway has a pivotal role in tumor suppression in humans.

Mdm2 and Mdm4 (also called Mdmx; human orthologues often referred to as Hdm2 and Hdm4, respectively) are structurally related proteins that serve as major negative regulators of p53.<sup>2–4</sup> They both contain an amino-terminal p53-binding domain, as well as a central acidic domain and a carboxy-terminal RING finger, and both are overexpressed in a variety of human tumors.<sup>2,4</sup>

Both Mdm2 and Mdm4 can bind to the transactivation domain of p53 and inhibit its transcriptional activity by physically blocking its interaction with components of the transcriptional machinery. In addition, Mdm2 is an E3 ubiquitin ligase that can drive polyubiquitylation and subsequent proteasomal degradation of p53.<sup>2,4</sup> Notably, the *Mdm2* gene is a positive transcriptional target of p53,<sup>5,6</sup> underpinning a negative feedback loop that tunes down cellular p53 activity. Although Mdm4 alone has no measurable E3 activity towards p53, the Mdm2-Mdm4 hetero-oligomer is a more efficient p53 E3 ligase than Mdm2 alone, and thus Mdm4 acts as an Mdm2-dependent enhancer of p53 degradation.<sup>7</sup>

microRNAs (miRNAs) are small non-coding RNAs, ~22-nt long, which regulate gene expression mainly through specific interaction with mRNA targets.<sup>8</sup> miRNAs are loaded onto the RISC complex to direct it to a specific subset of mRNAs, thus inhibiting their translation or targeting them for cleavage and degradation. Although miRNA binding sites are located throughout the length of the target mRNA, they are often found within the 3'UTR.<sup>8</sup> Not all putative miRNA binding sites are actually functional. One particular example is Alu sequences, which are primate-specific repetitive elements with more than one million copies in the human genome. Alu sequences present tens of thousands of potential miRNA targets, but most of those targets are ignored by the miRNA machinery and therefore have no impact.<sup>9</sup> Nevertheless, a small group of miRNA targets within Alus may become functional and may be retained when this is beneficial for the organism.<sup>9</sup>

miRNAs are intimately intertwined in the p53 pathway. Thus p53 regulates the expression of a substantial number of miRNAs, some positively and some negatively, and numerous components of the p53 pathway, including p53 itself, are subject to direct inhibitory regulation by specific miRNAs.<sup>10</sup> The fine balance between miRNAs and their mRNA targets within the p53 network is often perturbed in cancer.<sup>11</sup> In general, miRNAs that repress p53 activity will tend to be

<sup>1</sup>Department of Molecular Genetics, Weizmann Institute of Science, Rehovot, Israel and <sup>2</sup>Department of Molecular Cell Biology, Weizmann Institute of Science, Rehovot, Israel

\*Corresponding author: Y Pilpel, Department of Molecular Genetics, Weizmann Institute of Science, POB26, Rehovot 76100, Israel. Tel: +972 8 9346058; Fax: +972 8 9344108; E-mail: pilpel@weizmann.ac.il or

or M Oren, Department of Molecular Cell Biology, Weizmann Institute of Science, POB26, Rehovot 76100, Israel. Tel: +972 8 9342358; Fax: +972 8 9346004; E-mail: moshe.oren@weizmann.ac.il

<sup>3</sup>These authors contributed equally to this work.

**Keywords:** microRNA; p53; Mdm2; Mdm4

**Abbreviations:** miRNA, microRNA; WTP53, wild-type p53; DBD, DNA-binding domain; ER+, estrogen receptor positive; GOF, gain of function; FBS, fetal bovine serum; miR-661, miR-661 mimic; miR-C, miR-control mimic; si-miR-661, miR-661 inhibitor; si-miR-C, miR-control inhibitor; sip53, p53 siRNA

Received 07.7.13; revised 10.9.13; accepted 16.9.13; Edited by K Vouden; published online 18.10.2013

constitutively upregulated in cancer, whereas those that augment p53 activity, for example, by targeting Mdm2 or Mdm4, will tend to be silenced. Interestingly, polymorphisms that affect the recognition of particular p53 network transcripts by specific miRNAs may impact cancer progression, as exemplified by the case of Mdm4 and miR-191.<sup>12</sup>

Here we report that miR-661 targets simultaneously both *Mdm2* and *Mdm4* mRNA, at least in part via targets within Alu elements in their 3'UTRs, and increases the functionality of p53. Moreover, deregulated miR-661 expression may contribute to cancer in a manner that depends on p53 status.

## Results

**miR-661 downregulates simultaneously both Mdm2 and Mdm4.** To identify miRNAs that regulate the p53 pathway in human cells, we searched for miRNAs that are predicted to target multiple gene transcripts in the p53 network. Our prediction requested 7-mers within the target mRNA 3'UTR that fully match bases 2–8 of the particular miRNA. To increase the likelihood of true hits, we also requested that the specific miRNA will have more than one putative binding site within the 3'UTR of each target mRNA. Using these criteria, the strongest prediction was for miR-661 to target simultaneously the transcripts of human *Mdm2* and *Mdm4*, encoding two closely related major negative regulators of p53. Specifically, *Mdm2*'s 3'UTR contains three potential targets for miR-661, and *Mdm4* contains nine targets (Supplementary Figure S1).

To investigate whether miR-661 can indeed target Mdm2, we transiently transfected MCF7 breast cancer cells with miR-661 mimic. Although this led to only a slight reduction in *Mdm2* mRNA (Figure 1a), Mdm2 protein levels were markedly downregulated (Figure 1b). The effect of miR-661 on Mdm2 protein levels was reproduced in a variety of other cell lines, including A549 and H460 (non-small cell lung cancer), OVCAR-3 and OVCAR-8 (ovarian cancer), A375 (malignant melanoma) and MDA-MB-435 and MDA-MB-231 (breast cancer) (Figure 1b and Supplementary Figure S2). In most cases, p53 protein levels were not altered. Interestingly, while *Mdm2* mRNA levels were only marginally affected in MCF7 and A549 cells, a more significant reduction could be observed in MDA-MB-435 cells (Figure 1a). Notably, MCF7 and A549 express wild-type p53 (WTp53) whereas MDA-MB-435 express mutant p53. As Mdm2 downregulation is expected to increase the transcriptional activity of p53, and the *Mdm2* gene is a positive transcriptional target of p53, the negative effect of miR-661 on *Mdm2* mRNA may be partly compromised, in cells expressing WTp53, by increased transcription of the *Mdm2* gene. To address this possibility, we doubly transfected MCF7 cells with a combination of miR-661 mimic and p53 siRNA (sip53), thereby attenuating the Mdm2-p53 feedback loop. Indeed, depletion of p53 revealed a stronger downregulation of *Mdm2* mRNA by miR-661 (Figure 1c); in agreement, the decrease in Mdm2 protein was also more pronounced (Figure 1c).

Finally, to validate that endogenous miR-661 also targets Mdm2, we transfected MCF7 cells with miR-661 inhibitor. As seen in Figure 1d, this led to an increase, albeit modest, in

Mdm2. In sum, these observations identify Mdm2 as a *bona fide* target of miR-661.

As noted above, miR-661 is predicted to also target Mdm4. Indeed, transfection of MCF7 cells with miR-661 mimic elicited a modest reduction in Mdm4 protein (Figure 2), although we did not observe a significant effect on *Mdm4* mRNA (data not shown). Unlike its widespread effect on Mdm2, miR-661 did not suppress Mdm4 protein in several other cell lines (data not shown), suggesting that its ability to target *Mdm4* mRNA is highly context dependent. Conceivably, miR-661 may regulate Mdm4 in synergy with other miRNAs, expressed in MCF7 but not in the other cell lines examined. In fact, the *Mdm4* 3'UTR is exceptionally long and is predicted to harbor binding sites for a multitude of miRNAs.

Of the nine predicted miR-661 targets within the *Mdm4* mRNA 3'UTR, all except one reside within Alu repeats (Supplementary Figure S1). As Alu-embedded miRNA targets are often non-functional,<sup>9</sup> we surmised that the single non-Alu target was responsible for inhibition by miR-661. However, when cloned in a luciferase reporter, a 300-base-pair fragment spanning this target had no detectable effect in MCF7 cells (data not shown), as was also the case when several Alu-embedded putative targets were similarly tested individually. Thus, a combination of two or more targets may be required to mediate the inhibitory effect of miR-661 on Mdm4.

**miR-661 interacts with Mdm2 and Mdm4 mRNA within cells.** To obtain more direct evidence for the interaction of miR-661 with *Mdm2* and *Mdm4* mRNA, we performed an miRNA pull-down assay. Briefly, cells were transfected with biotinylated miR-661 mimic or miRNA control; biotinylated miR-661 retained the ability to downregulate both Mdm2 and Mdm4 (Figure 3b). Cell extracts were then prepared and reacted with streptavidin-coupled beads in order to affinity purify the miRNA mimic together with its associated mRNA molecules.<sup>13,14</sup> As seen in Figure 3a, both *Mdm2* and *Mdm4* mRNA were significantly enriched in the miR-661 pull-down relative to the miR-control pull-down; *Mdm2* mRNA displayed a greater fold enrichment than *Mdm4* mRNA. Actin mRNA, which is not a predicted miR-661 target, did not undergo comparable enrichment. These data strongly suggest that, as predicted computationally, miR-661 binds directly *Mdm2* and *Mdm4* mRNA.

**miR-661 augments p53 functionality.** Mdm2 and Mdm4 are both negative regulators of p53. Therefore, downregulation of Mdm2 and Mdm4 by miR-661 is expected to increase p53 functionality. One predicted manifestation is transcriptional activation of p53 target genes. We therefore monitored the impact of miR-661 overexpression on the endogenous levels of several such transcripts. Indeed, miR-661 overexpression significantly increased the amount of p21 mRNA, product of a canonical p53 target gene encoding a cyclin-dependent kinase inhibitor (Figure 4a). Consequently, p21 protein also increased (Supplementary Figure S3). Importantly, p21 induction was abolished by p53 knockdown (sip53, Figure 4a), confirming that the effect of miR-661 on p21 expression was p53 dependent. Comparable effects of miR-661 were also observed for additional p53 target genes,

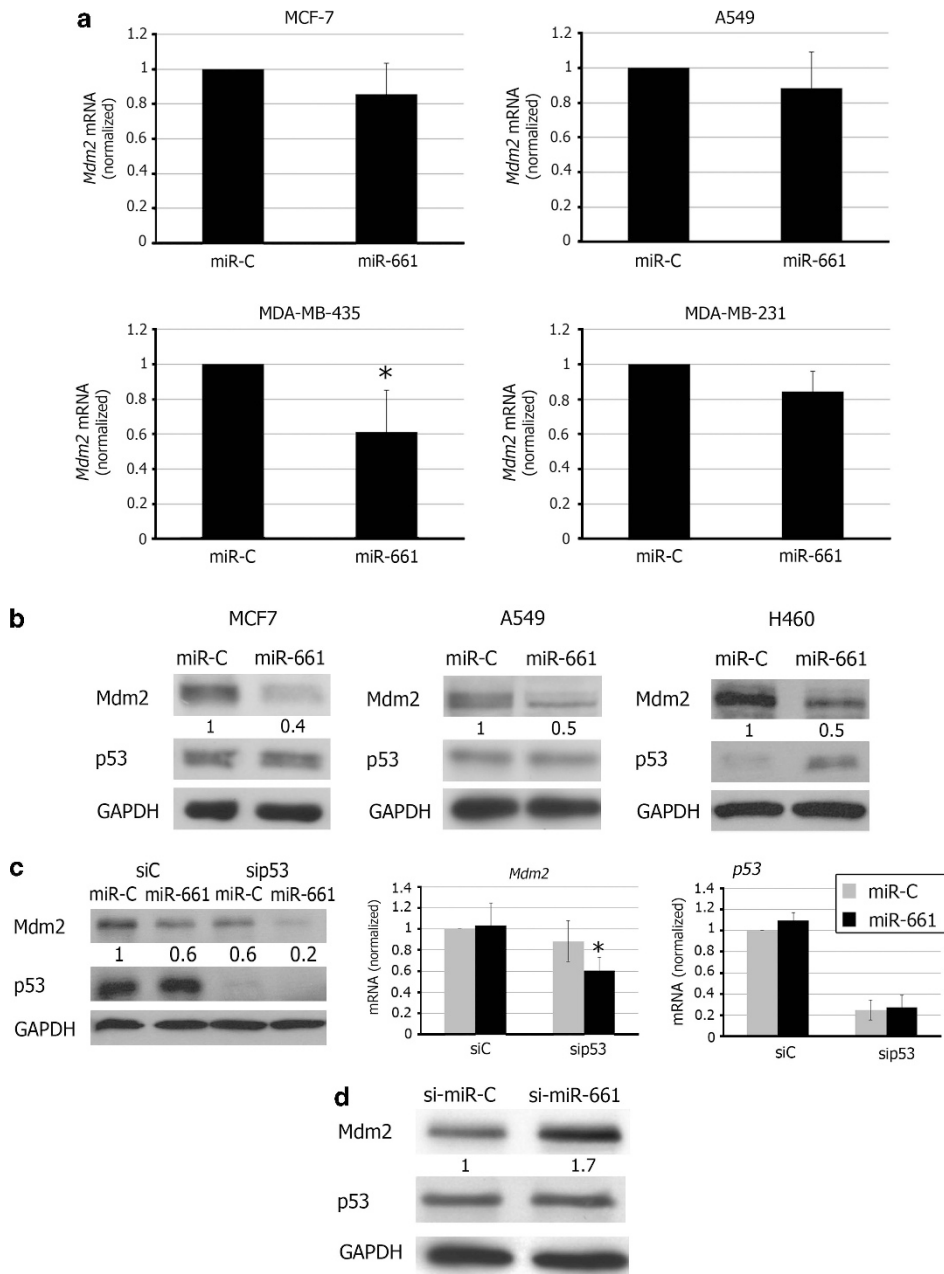


**Figure 1** miR-661 downregulates Mdm2. (a) The indicated cell lines were transfected with miR-661 mimic (miR-661) or miR-control (miR-C) (20 nM final) and harvested 48 h later for RNA extraction and qRT-PCR analysis of *Mdm2* mRNA. Values were first normalized to *GAPDH* (glyceraldehyde 3-phosphate dehydrogenase) mRNA in the same sample and then calculated relative to the miR-C value, set as 1. Values represent the average  $\pm$  S.D. from three (MCF7), two (A549), five (MDA-MB435) and four (MDA-MB-231) independent experiments. *P*-values for the difference between miR-661 and miR-C: MCF7 = 0.27, A549 = 0.6, MDA-MB-435 = 0.03, MDA-MB-231 = 0.1; Student's *t*-test. (b) Cells transfected as in (a) were lysed and subjected to western blot analysis with the indicated antibodies. Mdm2 band intensities were quantified. Values were first normalized to GAPDH intensities in the same sample, and then calculated relative to the miR-C value, set as 1. (c) MCF7 cells were transfected with miR-661 or miR-C (20 nM final) in combination with p53 siRNA (sip53; 20 nM) or control siRNA (siC; 20 nM). Forty-eight hours later, cells were harvested for western blot analysis with the indicated antibodies (left) or for RNA extraction and qRT-PCR analysis (middle and right panels) as in a and b. *P*-value for sip53 in the middle panel = 0.04; Student's *t*-test. (d) MCF7 cells were transfected with miR-661 inhibitor (si-miR-661; 100 nM) or miR-control inhibitor (si-miR-C), and harvested 48 h later for western blot analysis with the indicated antibodies. \**P* < 0.05

including *CD95*, *Btg2* and *Wig1* (Figure 4a). Moreover, miR-661 overexpression augmented the activity of a luciferase reporter gene driven by the p21 gene promoter (Figure 4b); a mutant version of this promoter lacking functional p53 binding sites (p21 MUT) was practically inactive. This further indicates that the increase in p21 mRNA after

transfection of miR-661 is due to upregulation of p53 transcriptional activity.

Intriguingly, despite reduced levels of Mdm2 and Mdm4 proteins following miR-661 overexpression, p53 protein levels did not increase noticeably in most cell lines (Figure 1b). This was at first glance puzzling, as a decrease in Mdm2 and

Mdm4 is expected to compromise p53 polyubiquitylation and therefore lead to p53 stabilization and accumulation, an expectation seemingly supported by the increased p53 activity (Figure 4). However, besides promoting p53 degradation, Mdm2 and Mdm4 also inhibit directly the biochemical

functions of p53.<sup>2</sup> We therefore reasoned that the relatively modest decrease in Mdm2 and Mdm4 might have been insufficient to elicit a detectable increase in p53 protein levels, yet was sufficient for augmenting p53's activity. To test this conjecture, we transfected MCF7 cells with low concentrations of *Mdm2* and *Mdm4* siRNA oligonucleotides and assessed the impact on p53 amount and activity. Indeed, the resultant mild decrease in Mdm2 and Mdm4, comparable to that achieved by miR-661 overexpression, did not affect p53 levels significantly (Supplementary Figure S4), but it nonetheless led to a visible increase in p21, attesting to functional p53 activation.

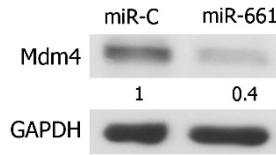


**Figure 2** miR-661 downregulates Mdm4. MCF7 cells were transfected with 20 nM miR-661 or miR-C and harvested 48 h later for western blot analysis with the indicated antibodies. Mdm4 band intensity was quantified and calculated relative to GAPDH (glyceraldehyde 3-phosphate dehydrogenase) in the same sample and to the miR-C value, set as 1

**miR-661 causes p53-dependent cell cycle arrest.**

To investigate the biological impact of p53 activation following miR-661 overexpression, we next examined the effect of this miRNA on the cell cycle. As seen in Figure 5a, transfection of MCF7 cells with miR-661 led to a significant decrease in the S phase fraction, monitored by BrdU incorporation. This effect was partially alleviated by knockdown of p53 (Figure 5a; knockdown validation in Supplementary Figure S5) and was reproduced with a different p53 siRNA (Supplementary Figure S6). Similar results were obtained in WTP53-expressing H460 and A549 cells (Figure 5a); in A549, both the inhibitory effect of miR-661 and its alleviation by p53 depletion were particularly pronounced. These data suggest that the cell cycle inhibitory effect of miR-661 is mediated by a combination of p53-dependent and p53-independent mechanisms. Remarkably, miR-661 did not affect cell cycle progression in ovarian carcinoma-derived OVCAR-3 cells (Figure 5b), which harbor a missense mutation in the p53 DNA-binding domain (DBD), or in OVCAR-8 cells that harbor a six amino acid in-frame deletion within the DBD<sup>15</sup> and are thus expected to have lost WTP53 function.

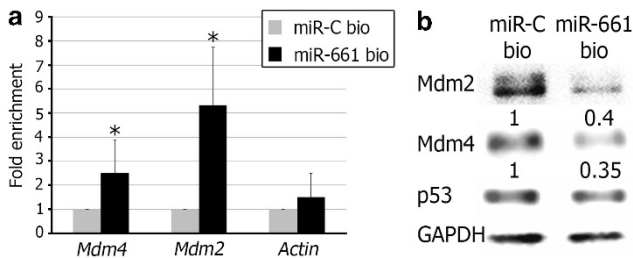


**Figure 3** miR-661 binds *Mdm2* and *Mdm4* mRNA within cells. (a) MCF7 cells were transfected with biotinylated miR-661 (miR-661 bio; 100 nM) or biotinylated miR-C (miR-C bio) and harvested 48 h later for pull-down analysis (see Materials and Methods). Fold enrichment with miR-661 relative to miR-C is shown for each indicated mRNA. Values represent the average  $\pm$  S.D. from five independent experiments. *P*-values for enrichment: *Mdm4* = 0.03, *Mdm2* = 0.002,  $\beta$ -actin = 0.3; one-tailed Student's *t*-test. (b) Extracts of cells processed as in (a) were subjected to western blot analysis with the indicated antibodies to validate the ability of miR-661 bio to downregulate Mdm2 and Mdm4. \**P* < 0.05

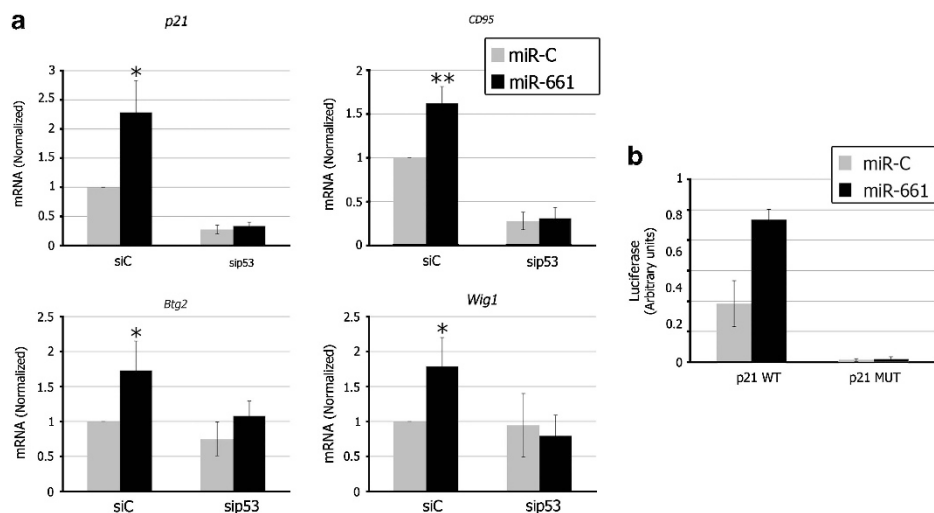


**Figure 4** miR-661 augments p53 transcriptional activity. (a) MCF7 cells were transfected as in Figure 1c. Forty-eight hours later, RNA was extracted and subjected to qRT-PCR analysis of the indicated transcripts. Values were calculated as in Figure 1a. Values represent the average  $\pm$  S.D. from 3–4 independent experiments. *P*-values for the difference between miR-661 and miR-C in the siC samples: p21 = 0.04, CD95 = 0.003, Btg2 = 0.05, Wig1 = 0.04; Student's *t*-test. (b) MCF7 cells were transfected with miR-661 or miR-control (20 nM final) for 48 h, followed by transfection of a luciferase reporter plasmid containing the wild-type *p21* promoter or a derivative thereof carrying p53 binding site mutations. Cell extracts were prepared 24 h later and subjected to luciferase analysis. A cotransfected plasmid expressing Renilla luciferase under the CMV promoter was used as a normalization control. \**P* < 0.05; \*\**P* < 0.01

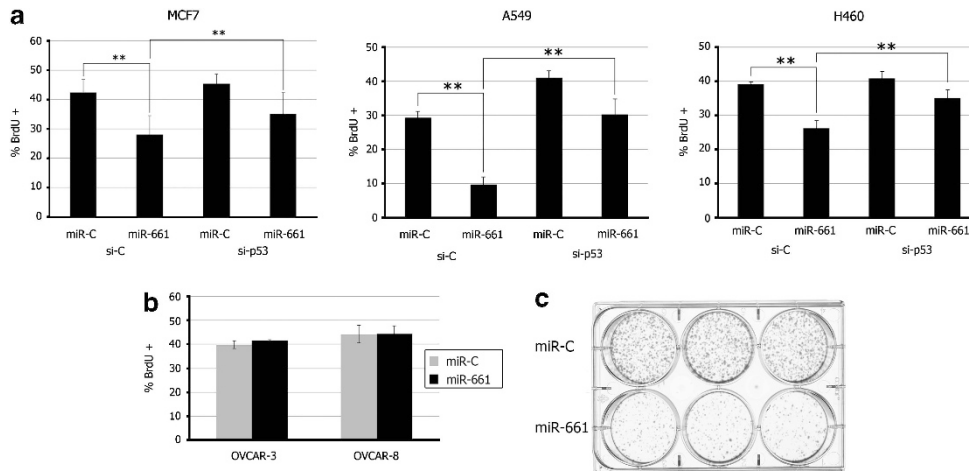


**Figure 5** miR-661 inhibits cell proliferation. (a) The indicated cell lines were transfected with miR-661 (20 nM) or miR-C for 48 h, followed by transfection of sip53 or siC. Twenty-four hours later, cells were subjected to bromodeoxyuridine (BrdU) incorporation analysis as described in Materials and Methods. The percentage of BrdU-positive cells is shown. Values represent the average  $\pm$  S.D. from 3–4 independent experiments. *P*-values for the indicated differences: MCF7 siC miR-661 versus siC miRC = 0.002, MCF7 miR-661 siC versus miR-661 sip53 = 0.003, A549 siC miR-661 versus siC miRC = 0.002, A549 miR-661 siC versus miR-661 sip53 = 0.002, H460 siC miR-661 versus siC miRC = 0.01, H460 miR-661 siC versus miR-661 sip53 = 0.005. (b) OVCAR-8 and OVCAR-3 cells were transfected with miR-661 (20 nM) or miR-C for 48 h and subjected to BrdU incorporation analysis as in (a). (c) MCF7 cells were transfected with 20 nM miR-661 or miR-C. Twenty-four hours later, cells were harvested and counted. Equal cell numbers were seeded for a colony-formation assay. Eight days later, cell colonies were fixed, stained and photographed. \*\**P* < 0.01

Consistent with its inhibitory effect on cell cycle progression in MCF7 cells, miR-661 overexpression also led to a reduction in long-term colony-formation capacity (Figure 5c). In conclusion, miR-661 overexpression can promote cell cycle arrest and reduce cell proliferation, at least partially through p53 activation.

**High miR-661 expression correlates with good prognosis in breast cancer.** As shown above, overexpression of miR-661 activates p53 and exerts antiproliferative effects in MCF7 cells. If this also holds true for actual tumors, one might predict that higher miR-661 expression may restrict tumor growth and aggressiveness, at least in cancer types that share similar features with MCF7. MCF7 are derived from an estrogen receptor positive (ER+) breast cancer; therefore, we used the MIRUMIR tool<sup>16</sup> to query the prognostic value of miR-661 expression levels in patients with high-risk ER+ breast cancers, based on published data.<sup>17</sup> As shown in the Kaplan–Meier plot in Figure 6a, patients with high miR-661 expression were found to have a better survival probability than low miR-661 expressors (*P*-Value = 0.0002). Of note, ER+ breast tumors have a very low rate of p53 mutations, and therefore mostly express WTp53.<sup>18</sup> This observation is consistent with our *in vitro* findings and suggests that reduced miR-661 expression may contribute to cancer aggressiveness, and possibly to therapy resistance, by attenuating p53 functionality in the tumor cells.

**The miR-661 locus is preferentially amplified in tumors with mutant p53 and miR-661 promotes migration of cells from such tumors.** Our data suggest that miR-661 may be considered a putative tumor suppressor, as it induces antiproliferative effects, partly through augmentation of p53 activity. Surprisingly, analysis of genome-wide *miR*-

661 locus alterations using the cBio portal<sup>19</sup> revealed that this locus actually tends to be amplified in a variety of cancers, including ovarian serous cystadenocarcinoma (~25% of cases) and invasive breast carcinoma (~7%) (Figure 6b). This might seem in disagreement with the proposed tumor-suppressive effects of miR-661; however, further analysis revealed that while only a minority of tumors included in this data set carried *TP53* gene mutations (Supplementary Figure S7; overall p53 mutation frequency in the entire set of tumors = 44%), in most tumors with miR-661 amplifications the *TP53* gene was actually mutated (Figure 6b). Remarkably, miR-661 amplification is particularly frequent in ovarian serous cystadenocarcinoma (Figure 6b), a tumor type with an exceptionally high rate of *TP53* gene mutations.<sup>20,21</sup> Hence, miR-661 amplifications appear to be largely avoided in tumors that retain WTp53, consistent with our prediction that, by boosting p53 functionality, such amplifications may interfere with tumor progression. Conversely, in tumors harboring p53 mutations, excess miR-661 may potentially become advantageous, favoring amplification of this locus.

Cancer-associated p53 mutations can endow the mutant p53 with cancer-promoting gain-of-function (GOF) activities.<sup>22,23</sup> Hence, in tumors harboring such mutations, miR-661 amplification might be favorably selected, because it may sometimes stabilize the mutant p53 protein and augment its GOF effects. This possibility is supported by an experiment where ovarian carcinoma-derived OVCAR-8 cells were transiently transfected with either miR-661 mimic or miR-661 inhibitor. OVCAR-8 cells carry a six nucleotide deletion within the p53 DBD and accumulate stable mutant p53 protein. As seen in Figure 6c, miR-661 overexpression led to a modest increase in mutant p53 levels. Moreover, miR-661 inhibition partially reduced p53 levels, suggesting that the endogenous miR-661 indeed contributes towards sustaining mutant p53 accumulation in those cells.

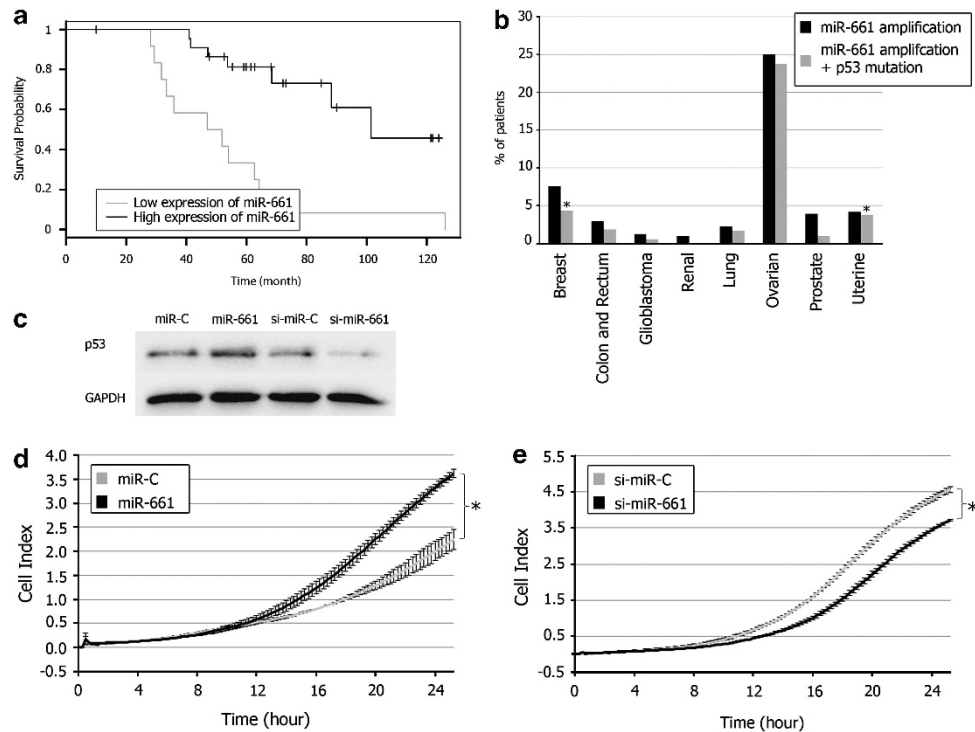


**Figure 6** miR-661 in cancer patients. (a) Kaplan–Meier survival curves for patients with ER + breast cancer expressing different miR-661 levels were calculated using the MIRUMIR tool. (b) For each cancer type, the overall percentage of patients with miR-661 genomic amplification, as well as the percentage of patients having both miR-661 amplification and p53 mutation, was calculated using the cBio portal. *P*-values for non-random association between p53 mutations and miR-661 amplification: breast invasive carcinoma = 0.015, colon and rectum adenocarcinoma = 0.7, glioblastoma multiformae = 0.1, renal clear cell carcinoma = 1, lung squamous cell carcinoma = 0.95, ovarian serous cystadenocarcinoma = 0.2, prostate adenocarcinoma = 0.2, uterine corpus endometrioid carcinoma = 6e-5; hyper-geometric distribution. (c) OVCAR-8 cells were transfected with 20 nM miR-661 or miR-control (miR-C) or with 100 nM miR-661 inhibitor (si-miR-661) or miR-control inhibitor (si-miR-C) and harvested 48 h later for western blot analysis with the indicated antibodies. (d) OVCAR-8 cells were transfected with 20 nM miR-C or miR-661 for 48 h, and then subjected to a real-time migration analysis as described in Materials and Methods. All experiments were conducted in three biological replicates. Representative data from one of the replicates is shown. A *t*-test was performed for the last time point of all three replicates, revealing significant (*P*-value = 0.02) differences in the means of the two populations. (e) OVCAR-8 cells were transfected with 100 nM si-miR-C or si-miR-661 for 48 h and analyzed as in (d). *P*-value = 0.04. \**P* < 0.05

One distinctive GOF activity of mutant p53 is augmentation of growth factor-induced cancer cell migration.<sup>24</sup> Indeed, depletion of endogenous mutant p53 markedly reduced serum-induced OVCAR-8 cell migration, confirming that the mutant p53 of these cells harbors GOF activities (Supplementary Figure S8). Importantly, miR-661 mimic overexpression significantly promoted OVCAR-8 cell migration (*P*-value = 0.02, Figure 6d; protein analysis in Supplementary Figure S9); conversely, miR-661 inhibition led to a modest but significant reduction in the rate of migration (*P*-value = 0.04, Figure 6e). Hence, in agreement with earlier findings,<sup>25</sup> miR-661 can augment the migration of cells harboring mutant p53. Overall, these findings are consistent with the observed amplification of miR-661 in serous ovarian cancer and suggest that such amplification might contribute to ovarian cancer progression partly through increasing mutant p53 levels.

## Discussion

In this study, we show that miR-661, a primate-specific miRNA, targets simultaneously two major negative regulators of p53: Mdm2 and Mdm4. In this manner, even very modest effects of miR-661 on each of these two proteins alone may translate into a significant effect on cellular p53 activity. It is

also noteworthy that most of the predicted miR-661 targets within the *Mdm2* and *Mdm4* RNA 3'UTRs reside within Alu elements; in fact, *Mdm2* has three predicted targets, all within Alus, while *Mdm4* has nine predicted targets, all but one within Alus. In general, miRNA targets within Alus tend to be non-functional.<sup>9</sup> However, there exist rare exceptions to this general rule, which might present an opportunity for the primate genome to acquire novel regulatory layers. Interactions of the primate-specific miR-661 with Alu elements within *Mdm2* and *Mdm4* mRNA may represent such an example.

Recent studies addressing the impact of miR-661 on cancer have yielded seemingly conflicting conclusions. Thus, one study concluded that miR-661 contributes to cancer aggressiveness, partly through inducing epithelial to mesenchymal transition;<sup>25</sup> the cell–cell adhesion protein Nectin-1 and the lipid transferase StarD10 were identified as the pertinent miR-661 targets. In contrast, others reported that miR-661 actually inhibits cancer progression and showed that its levels are strongly reduced as cells become more invasive;<sup>26</sup> in that study, metastatic tumor antigen 1 was identified as the pertinent miR-661 target. Our findings now offer a plausible resolution to this conundrum. We propose that in cells harboring WTP53, miR-661 will augment p53 functionality and therefore will be primarily tumor suppressive. In contrast, in cells that have acquired p53 mutations, miR-661 may

become pro-oncogenic. Indeed Reddy *et al.*,<sup>26</sup> who identified miR-661 as a putative tumor suppressor, used WTP53-positive MCF10A cells, whereas Vetter *et al.*<sup>25</sup> demonstrated elevated miR-661 expression in mutant p53-positive MDA-MB-435 and MDA-MB-231 cells, as compared with WTP53-expressing MCF7 cells. The findings presented here, in conjunction with the analysis of miR-661 alterations in various types of human cancer, further underscore the notion that the same miRNA may be either pro- or anti-tumorigenic, depending on cellular context. This duality is particularly striking in the case of breast cancer. In this cancer, miR-661 amplification is preferentially associated with *TP53* mutations (Figure 6b), prevalent in the more aggressive subclasses.<sup>18,27</sup> This stands in stark contrast with the fact that in breast cancer subclasses harboring mostly WTP53 high miR-661 expression can actually be shown to correlate with good prognosis (Figure 6a).

Notably, miR-661 resides within an intron of the *PLEC1* gene, encoding plectin, and the mature miRNA is presumably produced from processed *PLEC1* pre-mRNA. Interestingly, plectin is overexpressed in various human cancers and has been shown to promote cancer cell migration and invasion.<sup>28,29</sup> It is thus tempting to speculate that the embedding of miR-661 within the *plectin* gene may serve as a safeguard mechanism against aberrant overexpression of a potential oncogene. Thus, if excessive *PLEC1* expression is spuriously triggered by events such as gene amplification or transcriptional deregulation, miR-661 will be simultaneously induced, alerting p53 and preventing the potential oncogenic outcome of excessive plectin.

It is most certain that the diverse biological effects of miR-661 are dictated by much more than just p53 status. This is clearly illustrated by the fact that the cell cycle inhibitory effect of miR-661 overexpression is only partially alleviated by p53 depletion, and the extent of p53 dependence varies greatly among individual cancer cell lines (Figure 5a). Moreover, numerous additional targets beyond those described here and in previous studies<sup>25,26</sup> are expected to contribute to the diverse biological effects of miR-661. Identification of such additional targets and their possible crosstalk with the p53 pathway merits further investigation.

## Materials and Methods

**Cell culture, siRNA and miRNA transfections.** Cells were maintained at 37 °C in DMEM (Biological Industries, Beit-Haemek, Israel) supplemented with 10% heat-inactivated fetal bovine serum (FBS, Hyclone, Logan, UT, USA) (besides OVCAR-8 cells, which were maintained in RPMI with 5% heat-inactivated FBS) and penicillin–streptomycin antibiotics solution (Biological Industries).

Transient transfection of miRNA and siRNA was performed with Dharmafect 4 (MDA-MB-231) or Dharmafect 1 (all other cell lines) according to the manufacturer's (Dharmacon, Lafayette, CO, USA) instructions. miRNA mimics (Dharmacon) were used at a final concentration of 20 nM; siRNA (Dharmacon) was used at different concentrations. For RNA and protein analysis, Dharmafect Smart-pool siRNA was used. For cell cycle analysis, single siRNA oligos (Sigma, St. Louis, MO, USA and Dharmacon) were used. miRNA inhibitor (miRIDIAN microRNA Hairpin Inhibitor; Dharmacon) was used at 100 nM final concentration.

**RNA purification and real-time quantitative PCR.** RNA was extracted with the mirVana miRNA Isolation Kit (Ambion, Austin, TX, USA). For quantitative reverse transcriptase-PCR (qRT-PCR) analysis, 0.7–1.5 µg of each RNA sample was reverse transcribed with Moloney murine leukemia virus reverse transcriptase (Promega, Madison, WI, USA), random hexamer primers (Sigma) and dNTPs (LAROVA, Teltow, Germany). qRT-PCR was done in a StepOne

real-time PCR machine (Applied Biosystems, Foster City, CA, USA) with Syber Green PCR supermix (Invitrogen, Carlsbad, CA, USA).

**Primers.** The following primers were used (Sigma):

Gene	Forward primer (5'-3')	Reverse primer (5'-3')
p53	CCCAAGCAATGGATGATTGA	GGCATTCTGGGAGCTTCATCT
GAPDH	AGCCTCAAGATCATCAGCAATG	CACGATACCAAAGTTGTATGGAT
MDM4	AATGATGACCTGGAGGACTCTA	ACTGCCACTCATCCTCAGAGGTA
p21	GGCAGACCAGCATGACAGATT	GGGGATTAGGGCTTCTCTT
MDM2	CAGGCAAATGTGCAATACCAA	GGTTACAGCACCATTAGGTACAG
CD95	CCCTCTACCTCTGGTTCTTACG	TTGATGTCAGTCACTGGGCAT
Btg2	CCAGGAGGCACTCAGACAGC	GCCCTTGGACGGCTTTTC
Wig1	AGCTGTCTCTCTCTGCTAGAA	TCTGCGGAGGGACTGGAAC
Actin	CATGAAGATCAAGATCATCGCC	ACATCTGCTGGAAGGTGGACA

**Antibodies.** The following primary antibodies were used for western blot analysis.

GAPDH: monoclonal antibody Millipore MAB374; Mdm2: monoclonal antibodies 4B2, 2A9, and 4B11; Mdm4: BL1258 (Bethyl Laboratories, Montgomery, TX, USA); p53: monoclonal antibodies PAb1801 and DO1; and p21:c-19 (Santa Cruz Biotechnology, Santa Cruz, CA, USA).

**Western blot analysis.** For western blot analysis, cells were washed with PBS, collected and lysed with NP40 lysis buffer (150 mM sodium chloride, 50 mM Tris pH = 8, 1% NP40) with protease inhibitor cocktail (Sigma). Cells were vigorously vortexed and centrifuged at 14 000 r.p.m. for 10 min at 4 °C, and the soluble fraction was used to determine protein concentration in each sample. The protein concentration was quantified with the BCA kit (Thermo Scientific, Rockford, IL, USA) according to the manufacturer's protocol. Protein sample buffer (3% SDS, 10% glycerol, 5% β-mercaptoethanol, 62 mM Tris pH = 6.8) was added, and samples were boiled for 5 min and loaded onto SDS-polyacrylamide gels. Proteins were transferred onto nitrocellulose membranes, followed by 30 min blocking in 5% milk in PBS. The membranes were incubated with primary antibodies overnight at 4 °C, washed three times with PBS-T (0.05% Tween-20 in PBS) and reacted for 45 min with horseradish peroxidase-conjugated IgG, followed by three washes with PBS-T and one wash in PBS. The proteins were visualized using an enhanced chemiluminescence (ECL) detection kit (Amersham, GE Healthcare; Piscataway, NJ, USA), followed by exposure to X-ray film or analysis in a ChemiDoc MP imaging system (Bio-Rad). Bands were quantified with Image Lab 4.1 (BioRad, Hercules, CA, USA).

**Luciferase assays.** Cells were seeded in 12-well dishes and transfected with miRNA (20 nM final) as described above. Forty-eight hours later, cultures were transfected with 200 ng of firefly luciferase reporter plasmid DNA (p21 WT or p21 mutated) and 40 ng renilla luciferase plasmid DNA, using the JetPEI reagent (Polyplus Transfection, New York, NY, USA) in NaCl, according to the manufacturer's protocol. Twenty-four hours later, cells were washed twice in PBS and lysed with passive lysis buffer (Promega) for 15 min with shaking. Luciferase reporter activity was measured in a luminometer (Moduluc Microplate, Turner BioSystems, Sunnyvale, CA, USA).

**BrdU incorporation analysis.** Twenty-four hours after seeding, cells were transfected with miR-661 or miR-C (20 nM). Twenty-four hours later, cells were retransfected with 20 nM p53 siRNA (Sigma or Dharmacon single oligos) or LacZ siRNA (Dharmacon). After additional 24 h, cells were analyzed for BrdU incorporation as previously described.<sup>30,31</sup>

**Colony-formation assays.** Twenty-four hours after seeding, cultures were transfected with 20 nM miR-661 or miR-C. After additional 24 h, cells were counted, seeded in a six-well plate at a density of 3000 cells/well and incubated for 8 days at 37 °C in a humidified atmosphere of 5% CO<sub>2</sub>. The colonies were fixed with cold methanol for 5 min, stained with 0.1% crystal violet for 10 min and washed with distilled water.

**miRNA pull-down.** miRNA pull-down assays were performed as described.<sup>13,14</sup> MCF7 cells were seeded in 10-cm dishes 24 h before being transfected with biotinylated miR-661 mimic or miR control (100 nM; Dharmacon). After 48 h, cells were harvested in lysis buffer (20 mM Tris pH 7.5, 100 mM KCL,

5 mM MgCl<sub>2</sub> and 0.3% NP-40, including 100 μl/ml RNAse inhibitor (Promega) and Protease Inhibitor mix (Sigma) and incubated with Streptavidin Dynabeads (Invitrogen) for 4 h at 4 °C with constant rotation. The beads were prepared and washed according to the manufacturer's instructions, and incubated for 1 h at 4 °C with lysis buffer, including 1 mg/ml RNAse-free BSA and 1 mg/ml yeast tRNA (both from Ambion) before incubation with the lysed cells. After incubation with the beads, two washes with lysis buffer were performed and RNA was extracted with Trizol (Invitrogen) and Chloroform (Fisher Scientific, Waltham, MA, USA). cDNA preparation and qRT-PCR were done as described above, and values were normalized to input (cellular RNA without incubation with beads) and then to GAPDH.

**Cell migration analysis.** Cell migration was evaluated with the aid of a real-time cell analyzer (xCELLigence RTCA; Roche Applied Sciences, Mannheim, Germany), which provides a real-time measurement of migrating cells by extrapolating changes in electrical impedance with the number of cells passing through a porous membrane. Briefly, 160 μl of complete RPMI medium supplemented with 10% FBS (as attractant) were loaded in the lower chamber of the migration plate (CIM-Plate 16; Roche Applied Sciences). After fitting the upper chamber on the lower chamber, 35 μl of RPMI containing 0.1% FBS were loaded and allowed to equilibrate for 1 h in a 37 °C incubator.

A total of  $8 \times 10^4$  OVCAR-8 cells, transfected 48 h earlier with miR-C or miR-661 (20 nM) or with si-miR-C (miR-control inhibitor) or si-miR-661 (miR-661 inhibitor; 100 nM), were starved for 6 h in RPMI without FBS and then resuspended in 100 μl of RPMI containing 0.1% FBS. Then, cells were loaded in the wells of the upper chamber in the CIM-Plate (subsequently placed in the RTCA analyzer in a 37 °C incubator). After background reading was determined, cell migration was measured and recorded every 15 min (100 sweeps at 15-min intervals). RPMI medium without FBS loaded in the lower chamber was used as negative control. Each experiment was performed in three biological replicates.

**Clinical data analysis.** Data of miR-661 amplification and p53 status in patients from different cancers was generated using cBio portal (<http://www.cbioportal.org/public-portal/>).<sup>19</sup> For each cancer type, the percentage of patients with miR-661 amplification, p53 mutation or both together was calculated as an average of all data sets available for this cancer type. *P*-values were calculated with a hypergeometric distribution. Survival probabilities of breast cancer patients were generated with MIRUMIR (<http://www.bioprofiling.de/GEO/MIRUMIR/mirumirD.html>),<sup>16</sup> based on data taken from GSE37405.<sup>17</sup>

### Conflict of Interest

The authors declare no conflict of interest.

**Acknowledgements.** We thank Judy Lieberman for generous help with pull-down expertise, Debora Marks for bioinformatics ideas and Gilad Fuchs for the fruitful discussions. This work was supported in part by an FP7 grant 201102 (ONCOMIRS) from the European Research Council (to MO and YP), the 'Ideas' program of the European Research Council (to YP), grant R37 CA40099 from the National Cancer Institute (to MO), the Dr. Miriam and Sheldon G Adelson Medical Research Foundation (to MO), the Ben May Charitable Trust (to YP) and the Weizmann Institute Kahn Center (to MO and YP). MO is an incumbent of the Andre Lwoff Chair in Molecular Biology. YP is an incumbent of the Ben-May Professorial Chair.

1. Levine AJ, Oren M. The first 30 years of p53: growing ever more complex. *Nat Rev Cancer* 2009; **9**: 749–758.
2. Wade M, Li YC, Wahl GM. MDM2, MDMX and p53 in oncogenesis and cancer therapy. *Nat Rev Cancer* 2013; **13**: 83–96.
3. Hu W, Feng Z, Levine AJ. The regulation of multiple p53 stress responses is mediated through MDM2. *Genes Cancer* 2012; **3**: 199–208.
4. Li Q, Lozano G. Molecular pathways: targeting Mdm2 and Mdm4 in cancer therapy. *Clin Cancer Res* 2013; **19**: 34–41.

5. Barak Y, Juven T, Haffner R, Oren M. Mdm2 expression is induced by wild type p53 activity. *EMBO J* 1993; **12**: 461–468.
6. Wu X, Bayle JH, Olson D, Levine AJ. The p53-mdm-2 autoregulatory feedback loop. *Genes Dev* 1993; **7**: 1126–1132.
7. Linares LK, Hengstermann A, Ciechanover A, Muller S, Scheffner M. HdmX stimulates Hdm2-mediated ubiquitination and degradation of p53. *Proc Natl Acad Sci USA* 2003; **100**: 12009–12014.
8. Bartel DP. MicroRNAs: target recognition and regulatory functions. *Cell* 2009; **136**: 215–233.
9. Hoffman Y, Dahary D, Bublik DR, Oren M, Pilpel Y. The majority of endogenous microRNA targets within Alu elements avoid the microRNA machinery. *Bioinformatics* 2013; **29**: 894–902.
10. Hermekeing H. MicroRNAs in the p53 network: micromanagement of tumour suppression. *Nat Rev Cancer* 2012; **12**: 613–626.
11. Lujambio A, Lowe SW. The microcosmos of cancer. *Nature* 2012; **482**: 347–355.
12. Wynendaele J, Bohnke A, Leucci E, Nielsen SJ, Lambert I, Hammer S *et al*. An illegitimate microRNA target site within the 3' UTR of MDM4 affects ovarian cancer progression and chemosensitivity. *Cancer Res* 2010; **70**: 9641–9649.
13. Orom UA, Lund AH. Isolation of microRNA targets using biotinylated synthetic microRNAs. *Methods* 2007; **43**: 162–165.
14. Lal A, Thomas MP, Altschuler G, Navarro F, O'Day E, Li XL *et al*. Capture of microRNA-bound mRNAs identifies the tumor suppressor miR-34a as a regulator of growth factor signaling. *PLoS Genet* 2011; **7**: e1002363.
15. O'Connor PM, Jackman J, Bae I, Myers TG, Fan S, Mutoh M *et al*. Characterization of the p53 tumor suppressor pathway in cell lines of the National Cancer Institute anticancer drug screen and correlations with the growth-inhibitory potency of 123 anticancer agents. *Cancer Res* 1997; **57**: 4285–4300.
16. Antonov AV, Knight RA, Melino G, Barlev NA, Tsvetkov PO. MIRUMIR: an online tool to test microRNAs as biomarkers to predict survival in cancer using multiple clinical data sets. *Cell Death Differ* 2012; **20**: 367.
17. Lyng MB, Laenkhölm AV, Sokilde R, Gravgaard KH, Litman T, Ditzel HJ. Global microRNA expression profiling of high-risk ER + breast cancers from patients receiving adjuvant tamoxifen mono-therapy: a DBCG study. *PLoS One* 2012; **7**: e36170.
18. Sorlie T, Perou CM, Tibshirani R, Aas T, Geisler S, Johnsen H *et al*. Gene expression patterns of breast carcinomas distinguish tumor subclasses with clinical implications. *Proc Natl Acad Sci USA* 2001; **98**: 10869–10874.
19. Cerami E, Gao J, Dogrusoz U, Gross BE, Sumer SO, Aksoy BA *et al*. The cBio cancer genomics portal: an open platform for exploring multidimensional cancer genomics data. *Cancer Discov* 2012; **2**: 401–404.
20. Ahmed AA, Etemadmoghadam D, Temple J, Lynch AG, Riad M, Sharma R *et al*. Driver mutations in TP53 are ubiquitous in high grade serous carcinoma of the ovary. *J Pathol* 2010; **221**: 49–56.
21. Bernardini MQ, Baba T, Lee PS, Barnett JC, Sfakianos GP, Secord AA *et al*. Expression signatures of TP53 mutations in serous ovarian cancers. *BMC Cancer* 2010; **10**: 237.
22. Oren M, Rotter V. Mutant p53 gain-of-function in cancer. *Cold Spring Harb Perspect Biol* 2010; **2**: a001107.
23. Walerych D, Napoli M, Collavin L, Del Sal G. The rebel angel: mutant p53 as the driving oncogene in breast cancer. *Carcinogenesis* 2012; **33**: 2007–2017.
24. Muller PA, Vousden KH, Norman JC. p53 and its mutants in tumor cell migration and invasion. *J Cell Biol* 2011; **192**: 209–218.
25. Vetter G, Saumet A, Moes M, Vallar L, Le Bechec A, Laurini C *et al*. miR-661 expression in SNAI1-induced epithelial to mesenchymal transition contributes to breast cancer cell invasion by targeting Nectin-1 and StarD10 messengers. *Oncogene* 2010; **29**: 4436–4448.
26. Reddy SD, Pakala SB, Ohshiro K, Rayala SK, Kumar R. MicroRNA-661, a c/EBPα target, inhibits metastatic tumor antigen 1 and regulates its functions. *Cancer Res* 2009; **69**: 5639–5642.
27. Langerod A, Zhao H, Borgan O, Nesland JM, Bukholm IR, Ikdaahl T *et al*. TP53 mutation status and gene expression profiles are powerful prognostic markers of breast cancer. *Breast Cancer Res* 2007; **9**: R30.
28. Bausch D, Thomas S, Mino-Kenudson M, Fernandez-del CC, Bauer TW, Williams M *et al*. Plectin-1 as a novel biomarker for pancreatic cancer. *Clin Cancer Res* 2011; **17**: 302–309.
29. Katada K, Tomonaga T, Satoh M, Matsushita K, Tonoike Y, Kodera Y *et al*. Plectin promotes migration and invasion of cancer cells and is a novel prognostic marker for head and neck squamous cell carcinoma. *J Proteomics* 2012; **75**: 1803–1815.
30. Aylon Y, Ofir-Rosenfeld Y, Yabuta N, Lapi E, Nojima H, Lu X *et al*. The Lats2 tumor suppressor augments p53-mediated apoptosis by promoting the nuclear proapoptotic function of ASPP1. *Genes Dev* 2010; **24**: 2420–2429.
31. Golomb L, Bublik DR, Wilder S, Nevo R, Kiss V, Grabusic K *et al*. Importin 7 and exportin 1 link c-Myc and p53 to regulation of ribosomal biogenesis. *Mol Cell* 2012; **45**: 222–232.

Supplementary Information accompanies this paper on Cell Death and Differentiation website (<http://www.nature.com/cdd>)